the DGD and the theoretical PDF of τ_ω given in[6] are plotted as solid lines. A good match of experimental and theoretical data can be stated proofing the accuracy of the PMD emulation. Note, that the PMD emulator exhibits a PMD value of ≈80 ps since it is intended to be used for PMD compensator performance testing where high values are required.

The experimental setup is displayed in Fig. 2. Using an optical switch the output of the tunable laser source can be directed to the transmitters (Tx) for both transmission formats and the PMD measurement equipment. This allows precise measurements at exactly the same wavelength in a short time. In order to show signal distortions caused by higher order PMD only, we eliminate 1st order PMD by aligning the input state of polarization to the PSP. This is done by manually changing the input polarization with a polarization controller while monitoring the received eye diagram. This adjustment to receive the "best possible eye opening" can be regarded as a first order PMD compensator. A standard preamplified direct detecting receiver (Rx) is used in both cases and sensitivity penalties (BER of 10^{-9} with PRBS of $2^{11}-1$) are measured.

For both modulation formats the penalties (compared to each back-to-back case) versus 2nd order PMD parameter τ_ω are shown in Fig. 3. The penalties correspond to the same PMD situation; in some cases for the same 2nd order parameter value multiple measurements are performed at different wavelengths.

It can be observed in Fig. 3 (left) that the penalties for duobinary transmission are always lower than for binary. Even for very high 2nd order PMD values, e.g. 3500 ps^2 the penalty in the duobinary case does not exceed 3 dB whereas for binary a penalty of ≈12dB is measured. 2nd order PMD adds to or subtracts to residual chromatic dispersion.[5] Since no fiber based dispersion is considered in this experiment PMD induced chromatic dispersion can create negative penalty values (see Fig 3 (left)) for duobinary modulation (which is due to the typical duobinary property that the eye is widened for some increasing dispersion values!). In addition, the spectral energy of the duobinary signal is more concentrated at the center frequency (carrier frequency) or at the center PSP to which the signal is aligned to. Thus the depolarization effect caused by the frequency dependent rotation of the PSP is less affective than for standard on-off keying. In order to illustrate signal distortion caused by higher order PMD only, The eye diagrams depicted in Fig. 3 (right) were measured for a high PMD value of 3200 ps^2. Besides, the back-to-back eye diagrams of both modulation formats are also shown.

4. Conclusion

We study the effect of higher order PMD and show that using a bandwidth reduced modulation format—such as duobinary coding—is an effective way to decrease signal distortions caused by (residual) higher order PMD. Our experimental results link the actual higher order PMD to the observed system penalty and therefore a quantitative evaluation is possible.

References

1. F. Bruyère: 'Impact of First- and Second Order PMD in Optical Digital Transmission Systems'. Optical Fiber Techn., 2, 1996, pp. 269–280.
2. H. Buelow: 'System Outage Probability Due to First- and Second-Order PMD'. Photonics Tech. Letters, May 1998, 10, (5), pp. 696–698.
3. H. Buelow, F. Buchali, W. Baumert, R. Ballentin and T. Wehren: 'PMD mitigation at 10 Gbit/s using linear and nonlinear integrated electronic equaliser circuits', Electronics Letters, January 2000, 36, (2), pp. 163–164.
4. R. Noé et al.: 'Polarization Mode Dispersion Compensation at 10, 20, and 40 Gb/s with Various Optical Equalizers'. Journal of Lightwave Technology, September 1999, 17, (9), pp. 1602–1616.
5. L. Nelson, R. Jopson and H. Kogelnik: 'Polarization mode dispersion penalties associated with rotation of principles states of polarization in optical fiber', OFC 2000, Baltimore, ThB2-1.
6. F. Heismann: 'PMD: Fundamentals and Impact on Optical Communication Systems'. Short course, ECOC 1998, Madrid.
7. W. Kaiser, T. Wuth, M. Wichers and W. Rosenkranz: 'Reduced Complexity Optical Duobinary 10 Gb/s Transmitter Setup Resulting in an Increased Transmission Distance'. Photonics Technology Letters, August 2001, 13, (8), pp. 884–886.
8. S. Lanne, J.P. Thiery, F. Bruyère and D. Penninckx,: 'Phase-shaped binary transmission modulation format resistance to polarization mode dispersion', Colloquium on High Speed and Long Distance, 16/1–16/4, London 1999.
9. L. Pierre and J.P. Thiery: 'Comparison of resistance to polarization mode dispersion of NRZ and phase-shaped binary transmission format at 10 Gbit/s', Electronics Letters, February 1997, 33, (5), pp. 403–403.
10. S. Lanne, D. Penninckx, J.P. Thiery and J.P. Hamaide: 'Extension of polarization mode dispersion limit using optical mitigation and phase-shaped binary transmission', OFC 2000, Baltimore, ThH3-1.

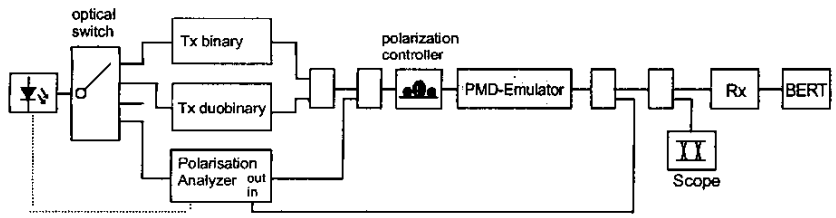

TuI5 Fig. 2. Test setup with conventional binary (NRZ) and duobinary transmitter (Tx), PMD emulator and standard preamplified receiver (Rx). The input polarization is adjusted to best case while monitoring the output eye.

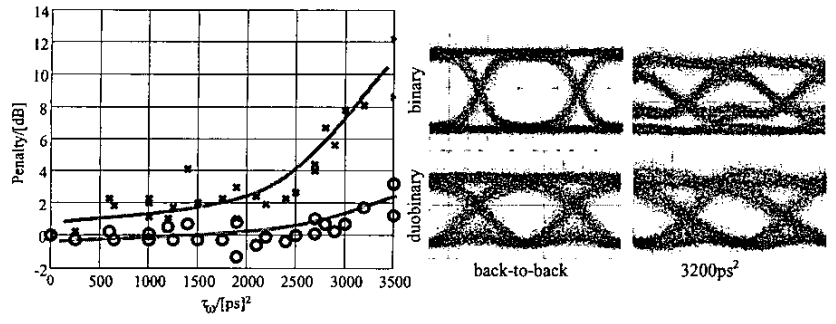

TuI5 Fig. 3. Measured Power Penalty vs. 2nd order PMD parameter τ_ω for binary (x) and duobinary (o) transmission (left); input polarization was aligned to the PSP in order to eliminate 1st order PMD effects. Eye diagrams of binary (top) and duobinary (bottom) at 10 Gb/s in the back-to-back case (left) and with signal distortion caused by higher order PMD only (right) with a 2nd order PMD value of 3200 ps^2.

TuI6 **3:15 pm**

Sensitivity Penalty distribution in fibers with PMD: a novel semi-analytical technique

Armando Vannucci and Alberto Bononi,
Dipartimento di Ingegneria dell'Informazione, Università degli Studi di Parma, viale delle Scienze 181A, 43100 Parma, Italy, Email: vannucci@tlc.unipr.it

Determining the Outage Probability (OP) of fiber communication systems in the presence of Polarization Mode Dispersion (PMD) requires long simulation times. For a given average Differential Group Delay (DGD) $\langle\Delta\tau\rangle$, sufficiently many fiber samples must be synthesized for propagation, so as to have fibers with first- and higher-order PMD effects large enough to degrade performance significantly. We choose here Sensitivity Penalty (SP), evaluated @BER = 10^{-10}, as the performance indicator. Since such *strong PMD* fibers are rarely synthesized, propagation on most fibers yields SP values falling close to the modal SP value. Hence, one gets a poor definition in the tail of the SP distribution. Recently, importance sampling techniques have been proposed to increase the definition in the tail.[1] Here, we take a different approach.

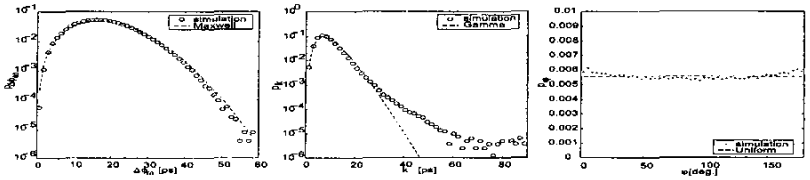

TuI6 Fig. 1. Marginal pdfs of the rotational model parameters ($\Delta\phi_\omega$, k, φ): simulation results (symbols); analytical approximations (dashed).

Given a method to classify synthesized fibers with respect to their all-order PMD effects by a finite set of parameters, one can perform propagation on only one sample among a subset of fibers with similar behaviour, i.e. with similar parameters values. This way, a *uniform sampling* of possible realizations in the fiber parameters space is accomplished. The joint distribution of the parameters employed for the classification is then used to give a weight to the evaluated SP data, according to the law of total probability. A good definition of the SP distribution in the tail is achievable, with significant savings in simulation time.

The rotational model

A fundamental issue in this work is the classification of simulated fibers based on a *rotational model* of the eigenmodes:[2,3] the Müller matrix of a fiber without polarization dependent loss can always be expressed in the form $M(\omega) = M(0)e^{\Delta\Phi(\omega)[\hat{b}(\omega)\times]}$, by factoring out its value at the reference frequency $\omega = 0$. The rotational model assumes $\Delta\phi(\omega) = \Delta\phi_\omega\omega$, i.e. that the retardation angle is linear in frequency, and that the eigenmode $\hat{b}(\omega)$ rotates in frequency at a constant angular speed κ around a fixed vector $\vec{k}$, i.e. it follows the equation of motion $\vec{b}_\omega(\omega) = \vec{k} \times \hat{b}(\omega)$, describing a cone with an aperture angle φ between $\vec{k}$ and $\hat{b}$. Such model, which implies nonzero all-order derivatives of the PMD vector $\vec{\Omega}(\omega) = \Delta\tau(\omega)\hat{q}(\omega)$, reliably represents the fiber Müller matrix over transmission bandwidths of the order of the inverse average DGD, as discussed in detail in.[2] Note that a simple relation links the *depolarization rate* of the PSPs $|\vec{q}_\omega|$, which is a second-order effect in PMD, and the rotational parameters:[3] $|\vec{q}_\omega| = 2k \sin\varphi$.

Estimation of parameters distribution

We synthesized 500,000 fibers with the standard Discrete Random Waveplate (DRW) model, using 100 plates, at an average DGD $\langle\Delta\tau\rangle = 18.4$ *ps*, and then fitted a rotational model to the Müller matrix of each fiber so as to determine the value of the parameters ($\Delta\phi_\omega$, k,φ). The value of $M(0)$, as well as the orientation of $\hat{k}$ and $\hat{b}(O)$ are irrelevant, since, for each fiber, propagation of signals with Input State Of Polarization (ISOP) uniformly covering the Poincaré sphere will be performed. The process of fiber synthesis and classification, that took 50 hours on a PC, yields the marginal probability density function (pdf) of the parameters shown in Fig. 1. We found that very good analytical approximations of the marginal densities i) $p(\Delta\phi_\omega)$, ii) $p(k)$ and iii) $p(\varphi)$ are i) a Maxwellian with mean value $\langle\Delta\tau\rangle$; ii) a Gamma distribution with mean value $\langle\Delta\tau\rangle/2$ and standard deviation $\langle\Delta\tau\rangle/4$; and iii) a uniform distribution. The dependence of such approximations, reported with dashed lines in Fig. 1, on $\langle\Delta\tau\rangle$ is a key feature: different sets of fibers with different values of $\langle\Delta\tau\rangle$ were simulated, yielding experimental evidence that both $p(\Delta\phi_\omega)$ and $p(k)$ *scale* with the average DGD, while $p(\varphi)$ is unchanged. Also, the bivariate and trivariate distributions of ($\Delta\phi_\omega$, k, φ), not reported here, indicate that there is a very weak correlation among these three parameters, so that $p(\Delta\phi_\omega)\,p(k)\,p(\varphi)$ is a satisfactory approximation of their joint pdf.

Building SP pdf

We now consider the three-dimensional space of the parameters ($\Delta\phi_\omega$, k, φ), within given parameters intervals, subdivided into equally spaced *cells:* we consider $\Delta\phi_\omega \in (0,60)$ *ps*, $k \in (0,90)$ *ps* and $\varphi \in (0,180)$ *deg.* (see Fig. 1), and divide such intervals in $n_{\Delta\phi}\omega = 18$, $n_k = 6$ and $n_\varphi = 6$ equally spaced bins, respectively, hence classifying the simulated fibers in 648 cells. Each cell is then associated to a finite probability, determined either as the relative frequency of synthesized fibers in the cell, or by integrating the analytical joint pdf given above. Note that, for $\langle\Delta\tau\rangle = 18.4$ *ps*, the 500,000 simulated fibers belong to 213 such cells only, hence about 2/3 of the cells are empty, in particular those associated both with large $\Delta\phi_\omega$ and large k values.

Performing extensive simulations of propagation of modulated signals on many ISOPs on all half million fibers would take months. We consider 213 *representative* DRW fibers only, each picked *at chance* inside each of the non empty cells. The transmitted signal is a 128-bit pseudo-random NRZ signal at 10 Gb/s, and, for each fiber, a set of SP values is obtained by propagating the input signal with 62 different ISOPs, which provide a uniform coverage of the Poincaré sphere. The SP histogram of each cell is weighted by the cell probability, then the whole set of weighted SP data is used to build the total SP pdf reported in Fig. 2(a). Formally, if $p(SP\,|\,\Delta\phi_{\omega i}, k_j, \varphi_l)$ is the conditional SP pdf, i.e. obtained from a particular fiber sample lying in the cell c_{ijl}, the global SP distribution is estimated by the law of total probability as:

$$p(SP) \cong \sum_{i=1}^{n_{\Delta\phi\omega}} \sum_{j=1}^{n_k} \sum_{l=1}^{n_\varphi} p(SP\,|\,\Delta\phi_{\omega i}, k_j, \varphi_l) P\{c_{ijl}\} \quad (1)$$

In Fig. 2(a), cell weights $P\{c_{ijl}\}$ are evaluated analytically from the product-form pdf. Using the relative frequency of fibers instead gives an SP pdf that is practically undistinguishable from that of Fig. 2(a).

Rotational fibers

The rotational model allows to synthesize a fiber Müller matrix with given parameters ($\Delta\phi_\omega$, k, φ) chosen to fit the matrix of a DRW fiber over a certain bandwidth. We repeated the whole signal propagation process on 648 rotational fibers, whose parameters are chosen *in the center* of each cell. The SP pdf evaluated by weighting the SP data obtained from propagation is also marked in Fig. 2(a) as "rotational model". The good match of the two curves (DRW fibers and rotational fibers) has a twofold implication: i) for each cell, the rotational model yields SP values that well approximate those of the corresponding DRW fiber, as verified numerically,[2] although the parameters of the rotational fiber lie in the cell center, hence are not fitted to the actual DRW fiber; ii) the SP distribution can be realiably evaluated using the rotational fibers, thus avoiding the time-consuming process of DRW fiber synthesis. Moreover, the rotational model allows synthesizing fibers with such parameters values, i.e. large $\Delta\phi_\omega$ and large k, that are too rare to be found in a pool of 500,000 samples of DRW fibers. The oscillations present in the SP pdf curves in Fig. 2(a) are an artifact of the discrete cell quantization, and get more and more attenuated as the cell resolution increases. Note that, given the rotational parameters, we have an expression of the fitted Müller matrix, and hence directly of the output intensity, while given the fitted PMD vector $\vec{\Omega}$ and its derivative $\vec{\Omega}_\omega$, one can only *approximate* the output intensity.[4]

In Fig. 2(a) we also report in dashed line the SP pdf obtained from synthesized fibers with first-order PMD only. In this case, the only free parameter is the DGD, and the same procedure as above was applied, using 18 synthesized fibers with equally spaced DGD values $\Delta\tau \in (0,60)$ *ps*. Note that a first-order PMD fiber corresponds to $k = 0$ in the rotational model: in this case $\Delta\tau(\omega) = \Delta\phi_\omega$ at any frequency ω. The fact that the pdf for large penalties is larger for the first-order PMD model is due to the fact that for the worst ISOPs the SP improves with moderate eigenmodes rotation.[3] Moreover, higher-order PMD is very sensi-

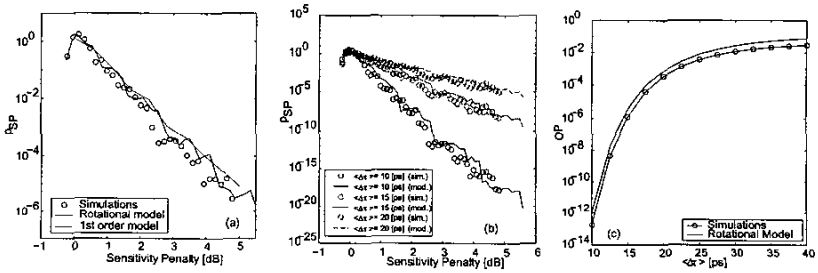

TuI6 Fig. 2. (a) pdf of Sensitivity Penalty obtained from: 213 simulated DRW fibers (symbols), 648 synthesized rotational model fibers (solid line), 18 synthesized first-order fibers (dashed line). (b) SP pdfs for different values of $\langle\Delta\tau\rangle$. (c) Outage Probability ($P\{SP > 3dB\}$) versus average DGD.

tive to the modulation format[5] and the use of RZ mark pulses instead of NRZ, may change the situation of Fig. 2(a).

Outage Probability

We define the OP as the probability that SP is larger than 3 *dB*. For an average DGD $\langle\Delta\tau\rangle = 18.4$ *ps*, integrating the pdfs obtained from both DRW and rotational fibers in Fig. 2(a), yields an OP equal to $1.5 \cdot 10^{-4}$ and $3.2 \cdot 10^{-4}$, respectively. When varying $\langle\Delta\tau\rangle$, the process of fibers simulation and classification needs not be repeated, since we can resort to the analytical joint pdf of the parameters $(\Delta\phi_\omega, k, \varphi)$ for the new average DGD. The same conditional probabilities appearing in[1] are now associated with a different weight. Hence, the same conditional SP data, already available from propagation performed on the previously selected fibers is re-used. As a consequence, similar statistical oscillations will be observed in the various SP pdfs derived with this method. Fig. 2(b) shows an example of how SP pdf varies for $\langle\Delta\tau\rangle = 10, 15, 20$ *ps*. Integrating the pdfs, we finally get the OP as a function of average DGD, reported in Fig. 2(c) for both DRW and rotational fibers. Note that, in a 10 Gb/s NRZ uncompensated system, an $OP = 10^{-5}$, i.e. five minutes per year of system outage, is achievable for an average DGD of about 15 *ps*.[6]

Conclusions

We proposed a novel semi-analytical technique for the evaluation of system outage probabilities in the presence of PMD at all-orders. Such technique relies on the rotational model for the fiber Müller matrix, whose rotational parameters were statistically characterized. Simulations of propagation can be performed either on a few hundred selected fibers or on a set of synthesized rotational models, to obtain reliable OP vs. average DGD curves, with significant gain in simulation time.

References

1. I.T. Lima Jr., G. Biondini, B. Marks, W.L. Kath and C.R. Menyuk, "Analysis of polarization-mode dispersion compensators using importance sampling," in *Proc. OFC 2001*, paper MO4-1 (2001).
2. A. Vannucci and A. Bononi, "The Rotational Model for all-order PMD," *submitted to OFC 2002.*
3. A. Bononi and A. Vannucci, "Is there Life beyond the Principal States of Polarization?," submitted for publication to *Optical Fiber Technol.*, (2001).
4. H. Bülow, "System Outage Probability Due to First- and Second-Order PMD," *IEEE Photon. Technol. Lett.* **10**, 696–698 (1998).
5. H. Sunnerud, M. Karlsson and P.A. Andrekson, "A Comparison Between NRZ and RZ Data Formats with Respect to PMD-Induced System Degradation," *IEEE Photon. Technol. Lett.* **13**, 448–450 (2001).
6. F. Roy, C. Francia, F. Bruyére and D. Penninckx, "A simple dynamic polarization mode dispersion compensator," in *Proc. OFC '99*, paper TuS4-1, 275–278 (1999).

TuI7 **3:30 pm**

Computation of the outage probability due to the polarization effects using importance sampling

I.T. Lima, Jr.,[1] A.O. Lima,[1] Y. Sun,[1] J. Zweck,[1] B.S. Marks,[1,2] G.M. Carter,[1,2] and C.R. Menyuk,[1,3] [1]*Department of Computer Sciences and Electrical Engineering, University of Maryland Baltimore County, Baltimore, MD, 21250; Email: lima@engr.umbc.edu;* [2]*Laboratory for Physical Science, College Park, MD, 20740;* [3]*PhotonEx Corporation, 200 Metro West Technology Park, Maynard, MA 01754*

A fundamental problem in the design of optical communication systems is to minimize channel outages due to the polarization effects. System designers commonly allocate a prescribed margin to polarization effects, such as 2 dB, with a certain probability that the margin will be exceeded, such as 10^{-6}. When this margin is exceeded an outage is said to occur. Because outages are so rare, it has been difficult to obtain them from experiments or from standard Monte Carlo simulations.

There are three polarization effects that lead to impairments in long-haul optical fiber transmission systems: polarization-mode dispersion (PMD), polarization-dependent loss (PDL), and polarization-dependent gain (PDG).[1,2] Since PMD, PDL, and PDG are slow time effects, it is reasonable to assume that they can be separated from the fast effects of nonlinearity and chromatic dispersion.[3] Wang and Menyuk validated this assumption and proposed the reduced Stokes model as a tool for the computation of the penalty induced by the polarization effects in long-haul transmission systems.[4] The reduced model only follows the evolution of the Stokes parameters and the average power of the signal and of the noise in each channel due to the combined effects of PMD, PDL, PDG, amplifier spontaneous emission noise, and the gain saturation of optical amplifiers. Thus, the reduced model applies when the PMD is not so large that it distorts the pulses within a single channel. We calculate the Q-factor from the signal-to-noise ratio[5] using a single fiber realization at a fixed level of PMD when PDL and PDG are present and when they are absent. From that, we may determine ΔQ (in dB) due to these effects. We note that only ΔQ is meaningful since the Q-factor does not contain the effects of chromatic dispersion and nonlinearity. We define the outage probability as the probability that ΔQ exceeds an allowed margin.

The reduced model decreases the computational time of simulations of the polarization effects by orders of magnitude when compared to full time domain simulations. Even so, until now efficient computation of outage probabilities as small as 10^{-6} has only been carried out using numerical extrapolation with a Gaussian function[4] to estimate the tails of the probability density function (pdf) of ΔQ obtained using Monte Carlo techniques in combination with reduced model simulations. In this contribution, we apply the technique of importance sampling[6] to resolve the tails of the pdf of ΔQ and thereby obtain a more accurate computation of the outage probability due to PMD and PDL. In addition, we have been able to determine the accuracy of the Gaussian extrapolation of the pdf of ΔQ. Importance sampling has been recently applied to the study of PMD emulators[7] and intra-channel PMD-induced distortions[8,9] in optical transmission systems.

To apply importance sampling, we first recall that P_I, the probability of an event defined by the indicator function $I(\mathrm{x})$, may be written as

$$P_I = \frac{1}{N}\sum_{i=1}^{N} I(\mathrm{x}_i)L(\mathrm{x}_i), \qquad (1)$$

where $L(\mathrm{x}) = p(\mathrm{x})/p^*(\mathrm{x})$ is the likelihood ratio, and $p(\mathrm{x})$ and $p^*(\mathrm{x})$ are the unbiased and biased density functions of the random vector x. The key difficulty in applying importance sampling is to properly choose $p^*(\mathrm{x})$. For a given channel, we have found that in order to bias towards large ΔQ values, the appropriate parameters to bias are the angles θ_n between the polarization state of the channel and the polarization state that undergoes the highest loss due to PDL in the n-th optical amplifier. The optical amplifiers are the main source of PDL in optical transmission systems. By biasing $\cos\theta_n$ towards one, we increase the likelihood that the ΔQ of the channel will be large. The angles θ_n are directly determined by the realization of the random mode coupling of the last birefringent section of the fiber that precedes the optical amplifiers. Thus, the values of $\cos\theta_n$ play the role of the components of the random vector x in Eq. (1). The indicator function I in Eq. (1) is chosen to compute the probability of having the value of ΔQ within a given range, such as a bin in a histogram. Thus, I is defined to be 1 inside the desired ΔQ range and 0 otherwise. Specifically, we select $\cos\theta_n$ using the same pdf used in:[9] $f(\cos\theta_n) = (\alpha/2)\,[(\cos\theta_n + 1)/2]^{\alpha-1}$, which corresponds to the unbiased case when $\alpha = 1$. With this pdf the likelihood ratio for each biased angle is given by $L(\cos\theta_n) = \alpha^{-1}\,[(\cos\theta_n + 1)/2]^{1-\alpha}$. Since the unbiased $\cos\theta_n$ are independent, the likelihood ratio of each realization of the system is equal to the product of the likelihood ratios of each biased angle. By varying α we can statistically resolve the pdf of the Q-factor in any desired range.

In order to compute outage probabilities using the reduced model we must first validate our implementation of the reduced model by comparison to a full time and frequency domain model using the Manakov-PMD equation.[10] We note that the importance sampling technique proposed here can also be applied to the full model. Figures 1.a and 1.b show numerical results of the mean of ΔQ in dB and its standard deviation, respectively, as a function of the PDL for each optical amplifier for the full and the reduced models. These results are for a trans-oceanic wavelength-division multiplexed (WDM) system with eight 10 Gbit/s return-to-zero channels spaced 1 nm apart. The total propagation distance is 8,910 km, with an amplifier spacing of 33 km, and 0.1 $\mathrm{ps/km^{1/2}}$ of PMD. There is no PDG in this example. For the full model the nonlinear coefficient n_2 is 2.6×10^{-20} $\mathrm{m^2/W}$ and the effective area is 80 $\mu\mathrm{m}^2$. The periodic dispersion map consists of one section of dispersion shifted fiber whose dispersion is −2 ps/nm-km at 1550 nm and whose length is 264 km, followed by a section of single mode fiber whose dispersion is 16 ps/nm-km and whose length is 33 km. In both sections the dispersion slope is equal to 0.07 $\mathrm{ps/nm^2}$-km. The residual dispersion in each of the channels whose central wavelength is not equal to the zero-dispersion wavelength is compensated for using symmetric pre- and post-dispersion compensation. Since the full simulations require a large amount of com-